World Academy of Science, Engineering and Technology
International Journal of Geotechnical and Geological Engineering
Vol:17, No:8, 2023

# Numerical Simulations of Frost Heave Using COMSOL Multiphysics Software in Unsaturated Freezing Soils

Sara Soltanpour, Adolfo Foriero



***Abstract*—**Frost heave is arguably the most problematic adverse phenomenon in cold region areas. It is a complex process that depends on heat and water transfer. The coupled physical fields generate considerable heave stresses as well as deformations. In the present study, a coupled Thermal-Hydraulic-Mechanical (THM) model using COMSOL Multiphysics in frozen unsaturated soils, such as fine sand, is investigated. Particular attention to the frost heave and temperature distribution, as well as the water migrating during soil freezing, is assessed. The results obtained from the numerical simulations are consistent with the results measured in the full-scale tests conducted by Cold Regions Research and Engineering Laboratory (CRREL).

***Keywords*—**Frost heave, numerical simulations, COMSOL software, unsaturated freezing soil.

## I. Introduction

IN this paper the emphasis is placed on frost heave which is generally defined as a vertical soil-surface displacement as a result of freezing. The primary cause of frost heave in the active layer is ice lensing. As a result of the frost heave process, the structure and mechanical properties of the soil are modified. This produces considerable damage to ground bearing structures such as pavement, pipes, piles, etc. [1]-[3].

In previous geotechnical engineering studies, excessive efforts have been made to investigate the freezing process in saturated and unsaturated soils both experimentally and theoretically [4]-[8]. Since unsaturated soils are generally found in most cold regions, the coupling of the mechanical, hydraulic and thermal regimes is necessary in order to get a realistic scenario of frost heave in unsaturated frozen soils. From here on, the problem encompassing heat and mass transport with respect to deformation and phase-change (i.e., freezing and thawing) is referred as the THM problem [5]. This entails the derivation of a system of governing partial differential equations along with the constitutive equations and the thermal, hydraulic and mechanical boundary conditions. THM problems, due to their nonlinear complexity, must be addressed with the finite element method. In past studies, some scientists developed and implemented theoretical models to simulate the coupled THM processes in freezing unsaturated porous materials [9]-[12].

Although there are numerous researches on the coupled THM process in unsaturated soils, less attention has been placed on fine sands.

This paper considers numerical simulations, using a theoretical coupled approach, with the COMSOL software for predicting frost heave in unsaturated freezing sands by comparison with full-scale freeze-thaw tests conducted at CRREL [13].

Sara Soltanpour is with the Departement de genie civil et de genie des eaux, Universite´ Laval, Pavillon Adrien-Pouliot, Quebec City, Quebec G1V 0A6, Canada (e-mail: sara.soltanpour.1@ulaval.ca)

Adolfo Foriero is an associste professor with the Departement de genie civil et de genie des eaux, Universite´ Laval, Pavillon Adrien-Pouliot, Quebec City, Quebec G1V 0A6, Canada (e-mail: adolfo.foriero@gci.ulaval.ca)

## II. THM Coupling Theory

A THM coupled theory of frost heave has been derived in the form of three governing partial differential equations. Subsequently, a finite element model of this coupled theory, with the COMSOL Multiphysics software, is utilized to numerically solve a system of governing nonlinear partial differential equations.

### *A. The Governing Equation of the Thermal Field*

The thermal field generally drives the frost heave process in frozen soils. Negative temperatures produce temperature gradients that induce frost heave deformation and water migration during the freezing process.

The partial differential equation with regards to the thermal field is defined as

$$(\rho C_p)_{eff}\frac{\partial T}{\partial t}+\rho C_p u\cdot\nabla T+\nabla\cdot q=Q \tag{1}$$

where ρ is the fluid density (kg/$m^3$), $C_p$ is the fluid specific heat capacity at constant pressure (J/K.kg), T is the temperature (K), u is the velocity field (m/s), q is the conductive heat flux (J/sec.$m^2$ or Watts/$m^2$) and $Q$ is the heat source (or sink) (J/sec.$m^2$ or Watts/$m^3$). Moreover, $(\rho C_p)_{eff}$ is the effective volumetric heat capacity of the solid-liquid system at constant pressure, defined as:

$$(\rho C_p)_{eff}=\theta_p\rho_p C_{p,p}+(1-\theta_p)\rho C_p+\frac{\rho L d\theta_p}{dT} \tag{2}$$

where $C_{p,p}$ is specific heat capacity at constant pressure of solid material in porous media (J/K.kg), $\rho_p$ is the density of the solid phase, ρ is the fluid density (kg/$m^3$), $C_p$ is the fluid specific heat capacity at constant pressure (J/K.kg), L is the

specific latent heat (for water ≈ 333.6 x $10^3$ J/kg), $\theta_p$ and 1- $\theta_p$ are volume fraction of solid and fluid in porous media, respectively.

In a continuous medium, Fourier's law of heat conduction states that the conductive heat flux (q), (J/sec.$m^2$ or Watts/$m^2$), is proportional to the temperature gradient via

$$q = -K_{eff} \nabla T \tag{3}$$

The effective thermal conductivity of the solid-fluid system, $K_{eff}$, is given as

$$K_{eff} = \theta_p k_p + (1-\theta_p) k \tag{4}$$

where $K_p$is thermal conductivity of the solid, $k$ is the thermal conductivity of the fluid (J/sec.(m.K) or Watts/m.K) and $\theta_p$ and 1- $\theta_p$ are volume fraction of solid and fluid in porous media, respectively.

*B. The Governing Equation of the Hydraulic Field*

Water flow in soil occurs due to driving forces associated with hydraulic gradients. In addition to this, temperature gradients generate hydraulic gradients in the unfrozen and frozen soils. These gradients produce movement of water towards the colder zones of the soil.

Darcy's law combined with the continuity equation of the porous medium gives a form of Darcy's Law for the interface:

$$\frac{\partial}{\partial t}(\varepsilon_P \rho) + \nabla \cdot (\rho(-\frac{k}{\mu}(\nabla P + \rho g \nabla D)) = Q_m . \tag{5}$$

By considering the time-derivative of (5) and by using the chain rule one obtains

$$\frac{\partial(\varepsilon_p \rho)}{\partial t} = \varepsilon_p \frac{\partial \rho}{\partial t} + \rho \frac{\partial \varepsilon_p}{\partial t} \tag{6}$$

and consequently

$$\varepsilon_p \frac{\partial \rho}{\partial t} + \rho \frac{\partial \varepsilon_p}{\partial t} = \varepsilon_p \frac{\partial \rho}{\partial P}\frac{\partial P}{\partial t} + \rho \frac{\partial \varepsilon_p}{\partial P}\frac{\partial P}{\partial t} . \tag{7}$$

If one defines the fluid compressibility as

$$X_f = (\frac{1}{\rho})(\frac{\partial \rho}{\partial P}), \tag{8}$$

then upon substitution in (6) this yields

$$\frac{\partial(\varepsilon_P \rho)}{\partial t} = \rho(\varepsilon_P X_f + \frac{\partial \varepsilon_P}{\partial p})\frac{\partial P}{\partial t} = \rho S \frac{\partial P}{\partial t} . \tag{9}$$

The definition of the storage coefficient, S, is generally defined by hydrologists as

$$S = \varepsilon_P X_f + \frac{\partial \varepsilon_P}{\partial p} . \tag{10}$$

Thus, the final governing equation of fluid flow in a porous medium is given by

$$\rho S \frac{\partial P}{\partial t} + \nabla \cdot (\rho(-\frac{k}{\mu}(\nabla P + \rho g \nabla D)) = Q_m \cdot \tag{11}$$

The storage coefficient, S, of (11) is computed with

$$S = \frac{\varepsilon_P}{K_f} + (\alpha_B - \varepsilon_P)\frac{1-\alpha_B}{K_d} \tag{12}$$

where $\varepsilon_P$ is the porosity of the medium, $K_d$is the drained bulk modulus, $K_f$, is the bulk moduli of the fluid (N/$m^2$), ($K_f = \frac{1}{X_f}$). Here, the parameter $\alpha_B$ is Biot-Willis coefficient, which relates the volume of fluid expelled (or sucked into) a porous material element to the volumetric change of the same element. Since Biot-Willis coefficient depends on the properties of the porous matrix, Biot-Willis coefficient of a soft porous matrix is close to 1 ($\alpha_B \approx 1$) and for a stiff porous matrix, it is close to $\varepsilon_P$ ($\alpha_B \approx \varepsilon_P$).

*C. The Governing Equation of the Stress Field*

Solid mechanics describes the stress-strain behavior of a body in response to different types of loadings. Here again constitutive models are necessary in order to model frozen soil behavior. The momentum conservation equation is given as

$$\nabla \cdot \sigma + F_v = \rho \frac{\partial^2 u}{\partial t^2} \tag{13}$$

where $\sigma$ is the Cauchy stress tensor in spatial formulation (N/$m^2$), $F_V$ is a force per unit volume (N/$m^3$), ρ is the mass density (kg/$m^3$), and u is the displacement vector ($m$). For the stationary case $\frac{\partial^2 u}{\partial t^2} = 0$ and

$$\nabla \cdot \sigma + F_v = 0 \cdot \tag{14}$$

The strain-displacement equation is defined by:

$$\varepsilon = \frac{1}{2}(\nabla u + \nabla u^T) \tag{15}$$

where $\varepsilon$ is the strain and $u$ is the displacement vector.

In COMSOL Multiphysics, there are two implementations of deformation that are available: the additive decomposition of strain or the multiplicative decomposition of the deformation gradient. These are applicable respectively to small and large strains. The additive decomposition of strains, in a geometrically nonlinear analysis, yields the inelastic strain as

$$\varepsilon_{inel} = \varepsilon_0 + \varepsilon_{ext} + \varepsilon_{th} + \varepsilon_{hs} + \varepsilon_{\rho l} + \varepsilon_{cr} + \varepsilon_{vp} \quad (16)$$

where $\varepsilon_0$ is the initial strain, $\varepsilon_{ext}$ is the external strain, $\varepsilon_{th}$ is the thermal strain, $\varepsilon_{hs}$ is the hygroscopic strain, $\varepsilon_{pl}$ is the plastic strain, $\varepsilon_{cr}$ is the creep strain and $\varepsilon_{vp}$ is the viscoplastic strain.

In a geometrically linear analysis, the elastic strain, $\varepsilon_{el}$, is computed by subtracting all inelastic strains, $\varepsilon_{inel}$, from the total strain, $\varepsilon$, based on the additive strain decomposition, which in the case of small strains gives

$$\varepsilon_{el} = (\varepsilon - \varepsilon_{inel}) \cdot \quad (17)$$

For an isotropic linear elastic material defined by a single Young's modulus, E, and Poisson's ratio, ϒ. Therefore, the tensors of stress, $\sigma$, (N/$m^2$ ) and strain, $\varepsilon$, are related via

$$\sigma = C : \varepsilon \quad (18)$$

In the COMSOL Multiphysics software, additional stress contributions, $\sigma_{ex}$, which are not part of the constitutive relations for describing strain-stress behavior, are added to the total stress tensor with:

$$\sigma = \sigma_{ex} + C : \varepsilon_{el} = \sigma_{ex} + C : (\varepsilon - \varepsilon_{inel}) \quad (19)$$

where $\sigma_{ex}$ is the additional stress contribution given as

$$\sigma_{ex} = \sigma_{ext} + \sigma_0 + \sigma_q \quad (20)$$

where $\sigma_0$ is the initial stress, $\sigma_{ext}$ is the external stress and $\sigma_q$ is the viscous stress occurring under material damping.

## III. FEM Simulations with COMSOL

In this section, a simulation of frost heave using a coupled THM approach is presented. Two experimental conditions conducted at CRREL are modeled with the COMSOL software: one experiment considers a shallow water table (wet case) with an average saturation of 87%, and the other a deep water table (dry case) with an average saturation of 40%.

The results of the simulations are then compared with full-scale freeze-thaw tests conducted at CRREL [13].

The simulations are conducted with the following assumptions:

- The material is assumed as isotropic.
- The material behavior is assumed as linear elastic.
- Vapor and ice flux are negligible.
- Darcy's law applies to water movement.

### *A. Initial and Boundary Conditions*

In order to create 3D model (see Figs. 1 and 2) with the multiphysics user interface in COMSOL, the following inputs are required:

- Element dimensions
- Thermal boundary conditions
- Hydraulic boundary conditions
- Mechanical boundary conditions
- Initial temperature and pore pressure with depth
- Initial displacement field

Finite element simulations are carried out with the commercial software COMSOL 5.6. A typical fine finite element mesh is shown in Fig. 2.

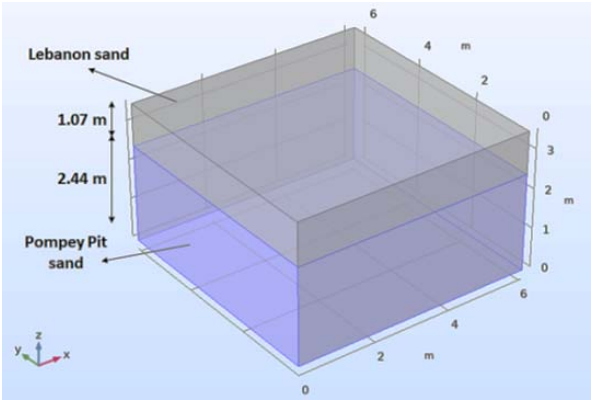


Fig. 1 3D model in COMSOL software

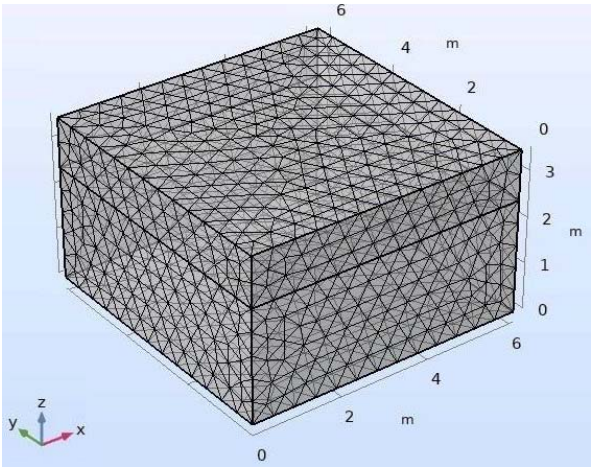


Fig. 2 FEM mesh for the 3-D model in COMSOL software.

The dimensions and boundary conditions of the FEM model are consistent with those of the experimental model at CRREL, and are as follows:

- The dimensions of the FEM model consist of a Lebanon sand layer (overall thickness 1.07 m) overlying a Pompey Pit sand layer (overall thickness 2.44 m) (see Table II).

- For the thermal boundary conditions, the upper boundary temperature is set to -12 °C as lowest temperature based on the CRREL experiments and all the other boundaries are considered as insulated.
- For the hydraulic boundary conditions, the pore water pressure of the upper boundary is set to 0 m of water (drained boundary condition) based on CRREL experiments and there is a no-flow condition for the other boundaries.
- For the mechanical boundary conditions, all boundaries except the upper-boundary are modeled as rollers.

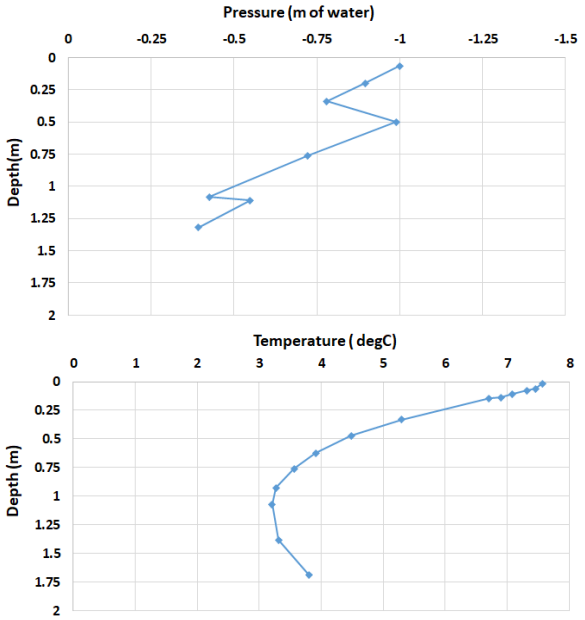


Fig. 3 Initial temperatures and pore water pressures for the dry case

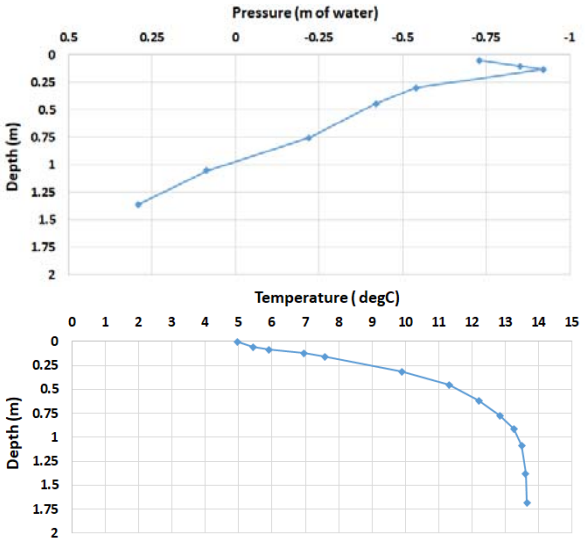


Fig. 4 Initial temperatures and pore water pressures for the wet case

The input of the initial values is realized with a set of specified graphs (shown in Figs. 3 and 4), indicating the initial values of temperatures and pore water pressures with depth for the dry and wet cases. These initial values were obtained in the experiments at CRREL. The initial displacement field with components u, v, and w is considered zero in this model.

### *B. Soil Parameters*

The soil parameters used in the present simulations were obtained from laboratory testing at CRREL and are presented in Tables I and II.

TABLE I
THERMAL PROPERTIES OF PHASES USED IN NUMERICAL SIMULATIONS

| Material | Specific Heat capacity $\left(\frac{Cal}{g(^{\circ}C)}\right)$ | Thermal conductivity $\left(\frac{Cal}{cm\ hr\ (^{\circ}C)}\right)$ |
|---|---|---|
| Water | 1 | 5 |
| Ice | 0.55 | 18 |
| Soil particles | 0.2 | 33.5 |

Cal= Calories, g = Gram, $^{\circ}C$ = Celsius degree, cm = centimeter, hr = hour.

### *C. Additional Physical Parameters*

The coefficients of thermal expansion, $\alpha(T)$, and the Young's modulus, E, were obtained from results obtained in the literature. When the interval of subfreezing temperatures nears 0 °C, then such temperature plays a significant role in engineering applications [14]. For example, for the sand in the temperature interval from -0.2 °C to -3.1 °C, the coefficient of thermal expansion $\alpha(T)$ is (-62.5 to -195) x $10^{-6}$ $1/^{o}C$. In the present simulation, $\alpha(T)$ = (-195) x $10^{-6}$ $1/^{o}C$.

The variation of Young's modulus, E, ($N/m^2$) with temperature is represented by empirical equations in [15].

For frozen sand at temperatures down to –10 ºC, the Young's modulus, E, of Lebanon sand and Pompey Pit sand can be calculated by

$$E = 500\left(1+4.2\,T_o\right) \tag{21}$$

where To is the number of °C below 0 °C and the Young's modulus (E) is given in MPa.

## IV. ANALYSIS OF RESULTS

### *A. Vertical displacement (Heave)*

Figs. 5 and 6 illustrate the predicted frost heave obtained by the FEM simulations versus the measured values of the CRREL experiments. In both of these figures, the magnitude of the simulated frost is well within that measured for the deep water table (dry case) and shallow water table (wet case).

During the experiments conducted at CRREL, frost heave was measured by undertaking level surveys of the test-tank soil surface. Specifically, measurements were taken on the last day of both the dry-freeze (Day 138) and wet-freeze experiment (Day 313). These measurements were then compared to the measurements taken before freezing at marked spots on the soil surface.

TABLE II
PHYSICAL AND HYDRAULIC SOIL PROPERTIES USED IN NUMERICAL SIMULATIONS

| Property | | Lebanon sand | | | Pompey Pit Sand |
|---|---|---|---|---|---|
| | | Layer 1 (0.0-0.15 m) | Layer 2 (0.15-.46 m) | Layer 3 (0.46-1.07 m) | |
| Soil density (kg/$m^3$) | | 1620 (Wet case) 1551 (Dry case) | 1678 | 1697 | 1978 |
| Soil porosity ( $m^3/m^3$) | | 0.419 | 0.419 | 0.419 | 0.336 |
| Soil water characteristics | $A_w$ | $1.962\times10^{-5}$ | $1.962\times10^{-5}$ | $1.962\times10^{-5}$ | $3.7116\times10^{-3}$ |
| | $\alpha_1$ | 1.975 | 1.975 | 1.975 | 1.268 |
| Permeability characteristics | $A_k$ | $1.590\times10^{-9}$ | $1.590\times10^{-9}$ | $1.590\times10^{-9}$ | $2.875\times10^{-5}$ |
| | $\beta_1$ | 4.623 | 4.623 | 4.623 | 3.806 |
| Min. unfrozen water content ( $m^3/m^3$ ) | | 0.03602 | 0.03602 | 0.03602 | 0.01787 |
| Saturated unfrozen hydraulic conductivity (x $10^{-6}$ m/s ) | | 4.448 | 4.448 | 4.448 | 15.29 |

m = Meter, kg = Kilogram, s = Second, $A_w$ and $\alpha_1$ = Gardner's multiplier and Gardner's exponent for the moisture characteristics, $A_K$ and $\beta_1$ = Gardner's multiplier and Gardner's exponent for hydraulic conductivity.

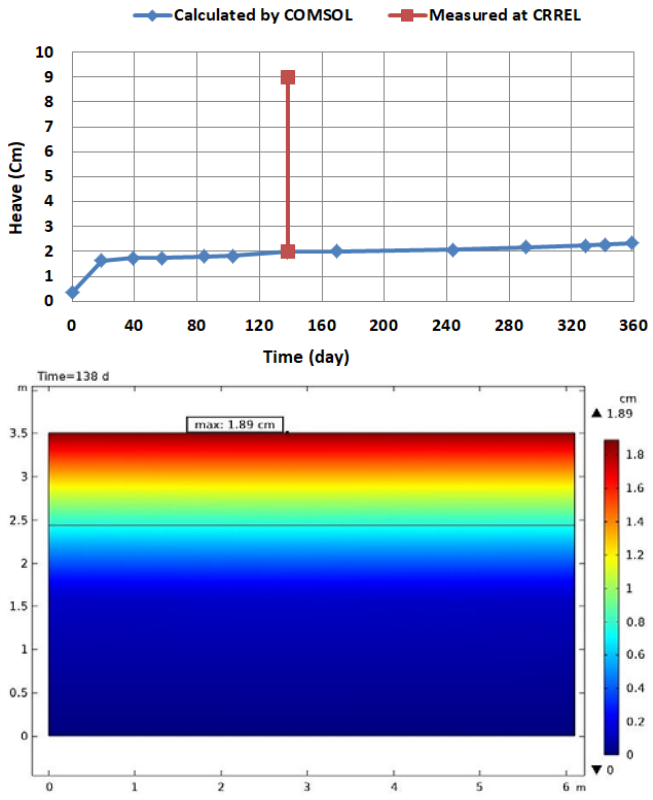


Fig. 5 Comparing predicted frost heave using COMSOL software with measured values during the test with deep water table

For the deep water table (dry case), the heave rate experiences a rapid non-linear increase of up to about 138 days. Subsequently the heave rate is significantly reduced, and after 200 days, it remains practically steady (see Fig. 5). Specifically FEM simulations yield a heave value of about 1.89 cm at day 138 while the range of heave measured is between 2 and 9 cm on the same and last day of the dry freeze experiment at CRREL.

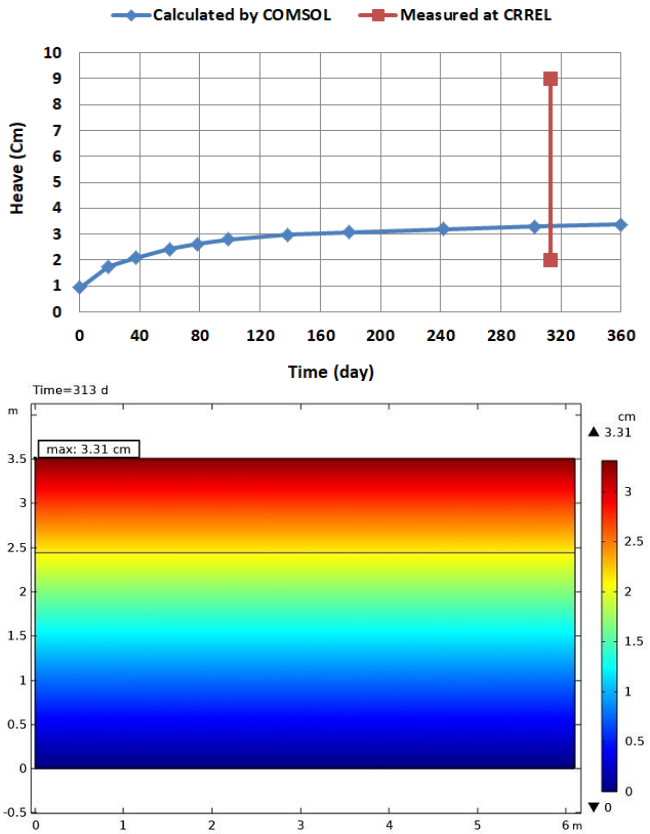


Fig. 6 Comparing predicted frost heave using COMSOL software with measured values during the test with shallow water table

For the shallow water table (wet case) simulation, a similar behavior is observable. Namely the heave rate experiences a rapid non-linear increase, but this time up to about 200 days (see Fig. 6). As shown in Fig. 6, the amount of heave increases, gradually attaining 3.31 cm at day 313, while the range of heave measured in the tests is between 2 and 9 cm on last day of wet freeze experiment at CRREL.

As a result, the net value of heave for the wet case is 3.31 cm at day 313 which is slightly greater than that for the dry case with a net value of 1.89 cm at day 138. This points to the fact that the heave rate decreases with the water table depth. Finally, it should be noted that the results obtained from the simulations are therefore consistent with the results measured at CERRL.

### *B. Temperature Distribution*

The changes of temperatures within the soil, for both dry and wet cases, over time are established in Figs. 7 and 8. During the freezing process, the figures show that the temperature obtained for both simulations drop gradually in different regions, with the exception of the case H = 2.975 m, during time. The reason is because this layer is close to the cold end, resulting in rapid temperature change which is better known as rapid cooling.

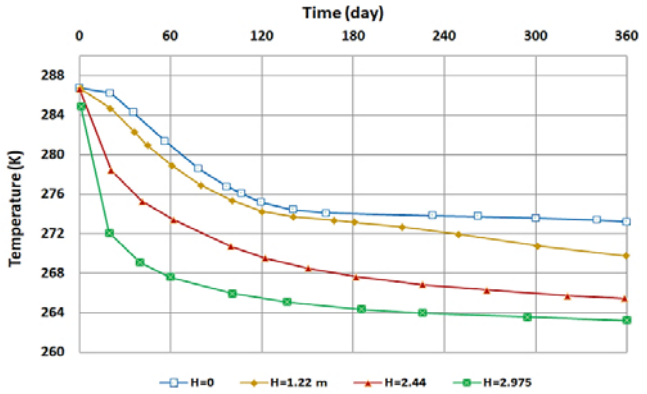


Fig. 7 Temperature Distribution at different times for the wet case

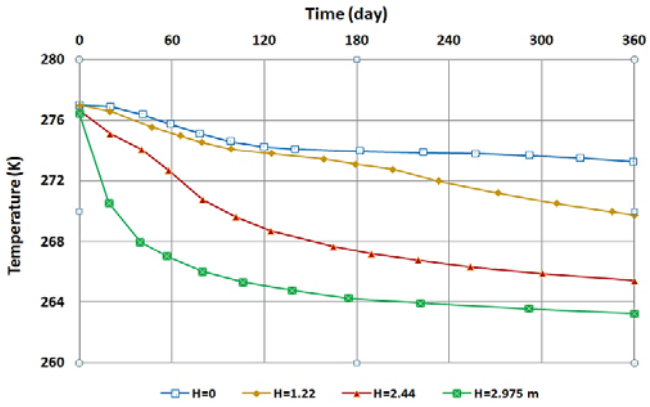


Fig. 8 Temperature distribution at different times for the dry case

The temperature gradient is an important factor for both water migration and frost heave. Figs. 9 and 10 show the variations of temperature gradient with time for both the shallow water table (wet case) and the deep water table (dry case) simulations, respectively.

For both the dry and wet case simulations, the temperature gradient has greater values for Lebanon sand than for Pompey Pit sand. As an example, for the shallow water table (wet case) simulation, the values are between 4 and 14 K/m for Lebanon sand, while for Pompey Pit sand the values are between 0 and 5 k/m. This makes sense since this layer is closer to the cold end.

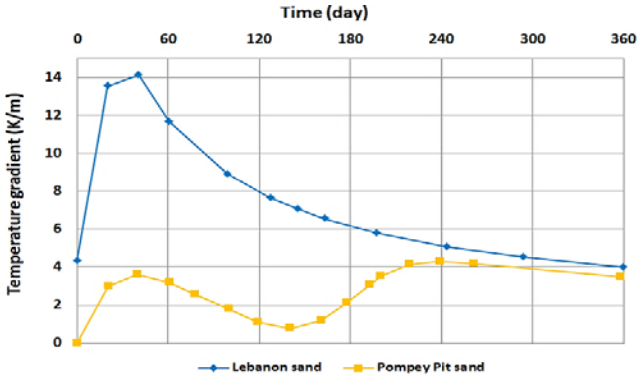


Fig. 9 Temperature gradient at different times for the wet case

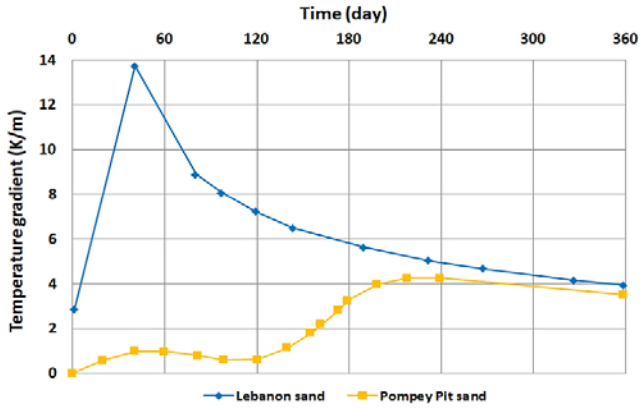


Fig. 10 Temperature gradient at different times for the dry case

## V. Water Migration

During the freezing process, the negative pore pressure draws the liquid water from the unfrozen soil towards the freezing front. Negative pore water pressure is synonymous to suction. Moreover, many experiments have indicated that the thermal gradient causes the pore water to migrate in the direction of lower temperatures [16].

As the freezing action continues, soil moisture transfers from the unfrozen region to the freezing front, which is the result of the interaction between temperature gradient and pore pressure gradient [16].

The ice lens prevents upward water migration, resulting in the changes in the structure of the pores and the properties of the water flow in freezing soil. In the unfrozen zone, the pore pressure is negative so that water is drawn to flow to the frozen areas [17].

For the shallow water table (wet case) simulation, the negative values of the pressure head (suction) decrease rapidly in Pompey Pit sand and Lebanon sand. The pressure head reach the positive amounts after 140 and 230 days in Pompey Pit sand and Lebanon sand, respectively (see Fig. 11).

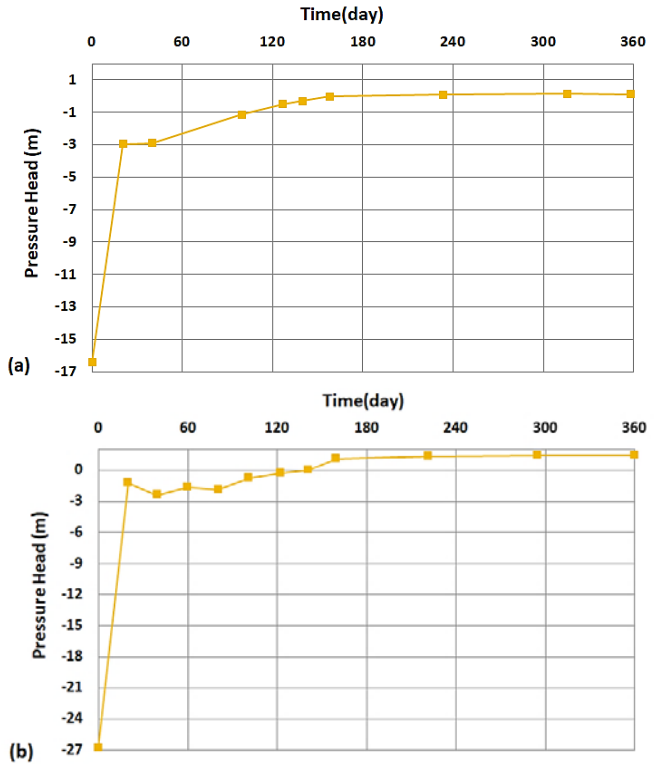


Fig. 11 Pressure Head versus time for the wet case: (a) Lebanon Sand and (b) Pompey Pit sand

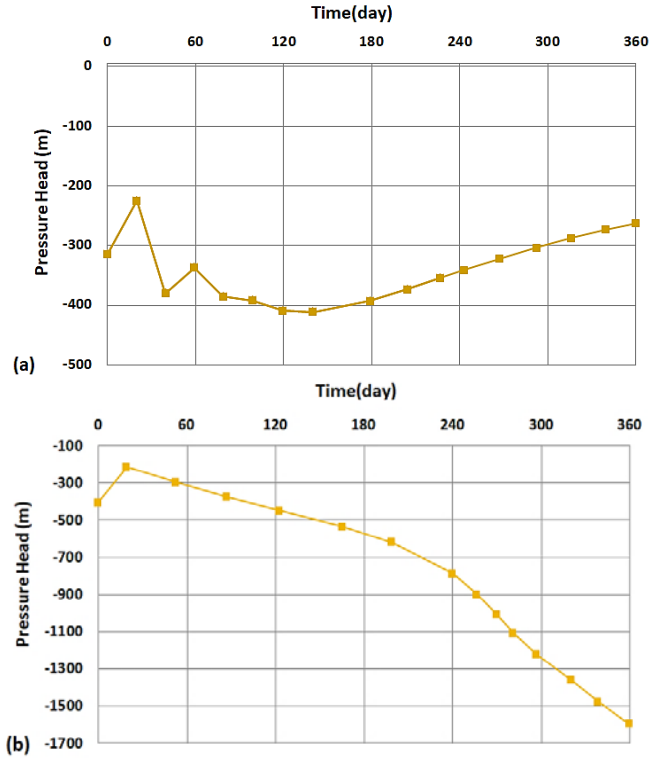


Fig. 12 Pressure Head versus time for the dry case: (a) Lebanon Sand and (b) Pompey Pit sand

For the deep water table (dry case) simulation, a different behavior is observable for Pompey Pit sand and Lebanon sand. For both Pompey Pit and Lebanon sand, the negative values of the pressure head do not attain the positive ones over time (see Fig. 12).

For the deep water table (dry case) and the shallow water table (wet case) simulation, the drainage of the unfrozen region occurs with the migration of water in the unfrozen region to the frozen region for both Lebanon and Pompey Pit sand.

The dominant factor affecting the pressure head is the location of the water table. For both Lebanon sand and Pompey Pit sand, the pressure head reaches the positive amount in shallow water table (wet case) due to the higher moisture content. On the other hand, the pressure head does not reach the positive amount in deep water table (dry case). The reason is that a decrease of moisture content produces suction in the unsaturated soil. Therefore, the negative value of pressure head for the deep water table (dry case) is higher than that in the shallow water table (wet case) for both Lebanon and Pompey Pit sand (see Figs. 11 and 12).

## VI. Conclusion

In this research, FEM simulations, using a theoretical coupled approach with the COMSOL software were considered. The reliability of this approach, in order to predict frost heave was assessed with comparison of full-scale tests conducted at CRREL. The system of coupled nonlinear partial differential equations was solved under experimentally measured initial and boundary conditions. As previously mentioned, the upper boundary temperature is set at a specified constant temperature.

Various conclusions were arrived based on the results of simulations with THM coupling. It is clear that the temperature gradient is responsible for water flow, resulting in the evolution of frost heave during the freezing process. During the first 40 days, frost heave progresses quickly due to the increased temperature gradient versus time for both the wet and dry cases. This is commonly known as the rapid progression stage. Subsequently, the transitional progression stage begins after 40 days. In this stage, the heave rate development slows down due to a decrease of temperature gradient with time. Finally, a stage of stability sets at day 180, where the heave rate gradually approaches zero. The reason is due to the formation of the ice lenses and unchanged temperature gradient. This renders water migration more difficult, and thus causes the rate of heave to be constant.

For future research, the upper boundary temperature will be set to a variable temperature as a function of time based on tests conducted at CRREL, in order to study frost heave and frost depth.

## References

[1] Foriero, A. and Ladanyi, B., (1994). *Pipe Uplift Resistance in Frozen Soils.* Journal of Cold Regions Engineering, ASCE, Vol. 8, No. 3, pp. 1-19

[2] Ladanyi, B. et Foriero, A., (1997). *Prediction of Adfreeze Frost Heaving Forces Acting on Piles.* Proceedings of the 50ième Canadian Geotechnical Conference, Ottawa.

[3] Ladanyi, B. et Foriero, A., (1998). *Evolution of Frost Heaving Stresses*

*Acting on a Pile*. Proceedings of the 7th International Permafrost Conference in Yellowknife, NWT, pp. 623-633.

[4] Philip, J.R. and Vries, D.A; (1957). *Moisture movement in porous materials under temperature gradient.* Trans. Am. Geophys. Union, 38, 222-232

[5] Snyder, V.A. and Miller, R.D; (1985). *Tensile strength of unsaturated soils.* Soil Sci. Soc. Am. J., Vol. 49, pp. 58-65.

[6] Jame, Y.W., and Norum, D.I; (1980). *Heat and mass transfer in a freezing unsaturated porous medium.* Water Resour. Res., Vol. 16, pp. 8 11 -81 9.

[7] Cary, J.W; (1965). *Water flux in moist soil: thermal versus suction gradients*. Soil Sci 100(3):168–175

[8] Cary, J.W; (1966). *Soil moisture transport due to thermal gradients: practical aspects.* Soil Sci Soc Am Proc 30(4):428–433

[9] Liang, Sihao; Teng, Jidong; Shan, Feng; Zhang, Sheng; Zhang; (2020). *A Numerical Model of Vapour Transfer and Phase Change in Unsaturated Freezing Soils*. Hindawi Advances in Civil Engineering, Volume 2020, Article ID 8874919.

[10] Liu, Z. and Yu, X; (2011). *Coupled thermo-hydro-mechanical model for porous materials under frost action: Theory and implementation.* Acta Geotech. 6, 51–65.

[11] Thomas HR, Cleall PJ, Li YC, Harris C, Kern-Luetschg M; (2009). *Modelling of cryogenic processes in permafrost and seasonally frozen soils.* Geotechnique 59(3):173–184

[12] Zhan, Y; Lu, Zh; Yao, H;(2020). *Numerical Analysis of Thermo-Hydro-Mechanical Coupling of Diversion Tunnels in a Seasonally Frozen Region*. J. Cold Reg. Eng., 2020, 34(3): 04020018

[13] Bigl, S.R. and Shoop, S.A; (1994).*Soil moisture prediction during freeze and thaw using a coupled heat and moisture flow model.* CRREL report 94-11, 1-19.

[14] Mordovskii, S.D., Vychuzhin, T.A. and Petrov, E.E; (1993). *Coefficients of linear expansion of freezing soils (translated from Russian).* Journal of Mining Science, 29: 39-42

[15] T. Sytovich, N. A and Swinzow, G.k.; (1975). *The mechanics of frozen ground*. Washington, DC, Scripta Book Co.; New York, etc., McGraw-Hill Book Co. (McGraw-Hill Series in Modern Structures.)

[16] Mageau, D. W. & Morgenstern, N. R ;(1980). *Observations on moisture migration in frozen soils.* Can. Geotech. J. 17, No. 1,54–60.

[17] Gilpin RR; (1980). *A model for the prediction of ice lensing and frost heave in soils.* Water Resour Res 16:918–930